

Production of Cu/Diamond composites for first-wall heat sinks

D. Nunes^{a,b}, J.B. Correia^b, P.A. Carvalho^{a,c}, N. Shohoji^b, H. Fernandes^a, C. Silva^a, L.C. Alves^d, K. Hanada^e, E. Ōsawa^f

^a*Associação Euratom/IST, Instituto de Plasmas e Fusão Nuclear - Laboratório Associado, Instituto Superior Técnico, Av. Rovisco Pais, 1049-001 Lisboa, Portugal*

^b*LNEG, Estrada do Paço do Lumiar, 1649-038 Lisboa, Portugal*

^c*ICEMS, Departamento de Engenharia de Materiais, Instituto Superior Técnico, Av. Rovisco Pais, 1049-001 Lisboa, Portugal*

^d*ITN, Instituto Tecnológico e Nuclear, Estrada Nacional 10, 2686-953 Sacavém, Portugal*

^e*National Institute of Advanced Industrial Science and Technology (AIST), 1-2-1 Namiki, Tsukuba, Ibaraki 305-8564, Japan*

^f*NanoCarbon Research Institute, AREC, Shinshu University, Tokida 3-15-1, Ueda, Nagano, 386-8567 Japan*

Due to their suitable thermal conductivity and strength copper-based materials have been considered appropriate heat sinks for first wall panels in nuclear fusion devices. However, increased thermal conductivity and mechanical strength are demanded and the concept of property tailoring involved in the design of metal matrix composites advocates for the potential of nanodiamond dispersions in copper. Copper-nanodiamond composite materials can be produced by mechanical alloying followed by a consolidation operation. Yet, this powder metallurgy route poses several challenges: nanodiamond presents intrinsically difficult bonding with copper; contamination by milling media must be closely monitored; and full densification and microstructural homogeneity should be obtained with consolidation. The present line of work is aimed at an optimization of the processing conditions of Cu-nanodiamond composites. The challenges mentioned above have been addressed, respectively, by incorporating chromium in the matrix to form a stable carbide interlayer binding the two components; by assessing the contamination originating from the milling operation through particle-induced X-ray emission spectroscopy; and by comparing the densification obtained by spark plasma sintering with hot-extrusion data from previous studies.

Keywords: copper; nanodiamond; interface reinforcement; carbide formation; spark plasma sintering.

1. Introduction

Copper alloys have been selected as first wall heat sinks due to their favorable thermal conductivity, mechanical strength and radiation resistance [1]. However, increased performance is demanded for operation temperatures above the range initially proposed for ITER [1]. This poses extra challenges especially on what thermal conductivity and mechanical strength are concerned, and alternative solutions are sought for long-term improvement. The extremely high thermal conductivity of diamond [2] turns its dispersions into excellent candidates for thermal management applications. Additionally, nanoparticle dispersions can be used as reinforcement for increased strength and thermal stabilization of the microstructure. Furthermore, Cu-diamond composites will also exhibit lower thermal expansion [3,4] mismatch with plasma facing W-based materials than copper alloys.

Dispersions of nanodiamond (nDiamond) in copper offer therefore great potential for first-wall heat sinks and can be easily produced by mechanical alloying. Previous studies have demonstrated that Cu-microdiamond composites present enhanced thermal conductivity [3,5]. Furthermore, high microstructural and thermal stability have been demonstrated for dispersions of nanodiamond in copper [4]. However,

processing of these nanostructured materials present several challenges:

(i) Diamond presents intrinsically difficult bonding with copper [6]. Yet chromium incorporated in the copper matrix can improve its adhesion to diamond and provide enhanced thermal coupling. Chromium tends to segregate to the reinforcement/metal interfaces, forming a stable carbide interlayer that leads to enhanced heat and load transfer between the composite components. Indeed, thermal conductivities as high as 50% above that of pure copper, have been achieved for Cu-carbide-microdiamond composites, and carbide interlayers are assumed to aid the electron-phonon coupling necessary for heat transfer [6].

(ii) Mechanical alloying (MA) is a well-known processing technique used to produce nanostructured composites [7]. However, one of its drawbacks is contamination arising from the milling media. This contamination can be minimized with appropriate milling parameters, but must be carefully monitored with high sensitivity techniques such as particle-induced X-ray emission (PIXE) spectroscopy.

(iii) Consolidation of mechanically alloyed materials is usually carried out by hot isostatic pressing (HIP) or by hot deformation [7,8]. However, these techniques tend to induce microstructural coarsening with a concomitant decrease in the material strength. The recently developed spark plasma sintering (SPS)

[9] is an alternative consolidation technique in which local heating resulting from intergranular plasma pulses enhances the mass transport at the powder particle surface (as required for sintering), while keeping the particle bulk at lower temperature.

The current research line aims to systematize the suitable processing conditions for Cu/nDiamond composites to be employed as heat-sinks integrated in first-wall panels. Powder mixtures of Cu/nDiamond were mechanically alloyed using chromium doping. Milling media contamination was monitored by PIXE. Heat treatments were used to assess the microstructure thermal stability. The densification and hardness results obtained with the SPS consolidation were compared with hot extrusion data from previous studies. Structural characterization was carried out by transmission electron microscopy (TEM) and X-ray diffraction (XRD).

2. Materials and methods

Powder mixtures of Cu:nDiamond in 90:10 proportion (10 at.% nDiamond) were mechanically alloyed with 0.1 wt% Cr following reference [10]. The nDiamond powder was prepared by stirred-media milling as previously reported [11], after evaporating the water from the colloid at 65°C for 24 h to remove 99% of water, which resulted in agglomerates with diameters of 2-3 μm . Pure elemental Cu was used as matrix (99.95% purity with particle size in the 44-149 μm range). Cr doping was carried out by incorporating in the mill charge the suitable proportion of a water atomized Cu-2.6 wt% Cr alloy powder [12].

MA was performed in a Retsch PM400 planetary ball mill operated at 400 rpm. The mill container was charged with 20 g of the above mixture and 400 g of hardened stainless-steel balls with a diameter of 10 mm. In order to prevent oxidation, the container was filled with argon. Different batches have been produced with 1,2,4,6 and 8h milling times. A control batch without Cr doping was produced for a milling time of 4h. The nDiamond dispersion was monitored through microstructural observations. The 4h as-milled Cu/Cr/nDiamond powder was annealed at 400°C and 600°C for 1 h in a tubular furnace under an argon flow. Due to the homogeneous dispersion achieved with 4 h this as-milled powder was subsequently consolidated by SPS at 800°C under a load of 400MPa for 3 min.

The mechanically alloyed, heat-treated and consolidated materials were characterized by XRD using Cu $K\alpha$ radiation to determine the average crystallite size of copper. The evaluation was performed from the highest intensity low angle Bragg reflections using Scherrer's equation.

Microstructural observations were carried out after standard metallographic preparation by scanning electron microscopy (SEM) in backscattered electron mode (BSE) with a FEG-SEM JEOL7001 instrument equipped for energy dispersive X-ray spectroscopy (EDS). TEM observations were performed with a Hitachi H8100 microscope equipped for EDS. The TEM samples were thinned to electron transparency by

argon ion milling using a Gatan-Duo Mill machine, operating at an acceleration voltage of 4 kV, with a 14° incidence angle.

Contamination of the mechanically alloyed materials was evaluated by PIXE. The experiments were carried out with 2.0 MeV proton beams of $\sim 3 \times 3 \mu\text{m}^2$ and a Si(Li) detector. The X-ray peak area determination and the quantitative analysis were performed with the AXILV3.0 and DATPIXE codes [13,14].

Microhardness was measured with a Vickers indenter using a Shimadzu HMV 2000 hardness tester with a load of 0.245 N and a dwell time of 15 s.

Density measurements were performed by the Archimedes method.

3. Results and discussion

Fig. 1 shows the variation of Cu crystallites size with milling time, heat treatment and consolidation for the Cu/Cr/nDiamond nanocomposites. The crystallite size decreased with milling time presenting values ranging from 18 nm to 27 nm. These results suggest that the nanodiamond particles contributed to break up the copper crystallites, acting as milling agents. The heat treatments and SPS consolidation resulted in modest grain growth. This result is remarkable since exposure of nanostructured pure copper to such high temperatures, even for short periods, leads to considerable microstructural coarsening and deterioration of the mechanical properties [15-17].

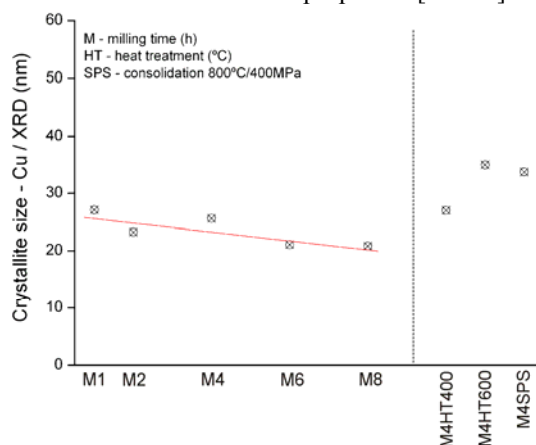


Fig. 1 Crystallite size of Cu/Cr/nDiamond nanocomposites. As-milled powders for milling times of 1h/2h/4h/6h and 8h, heat-treated powders at 400 and 600°C, and SPS consolidated sample.

Fig. 2 presents the microstructure of Cu/Cr/nDiamond powder milled for 8h. Microstructural homogeneity and extensive nDiamond dispersion were inferred from SEM observations for milling times higher than 4h. However, the number of Fe,Cr-inclusions originating from the milling media (see Fig. 2) also increased with milling time. Fig. 3 presents an EDS spectrum of a typical inclusion. As a result, the 4h milling batch was selected as an optimized dispersion vs contamination condition and the resulting powder was further used for heat treatments and consolidation.

Table 1 shows the average chemical composition determined by PIXE for the 4h milling condition. The

ratio Cr/Fe (0.218) exceeds the nominal ratio of the stainless steel milling media (0.159) with the difference originating from the Cr doping.

Fig. 4 presents the microstructure of the Cu/Cr/nDiamond material milled for 4h and annealed at 600°C. The heat-treatments were used to promote a fine carbide precipitation at the interfaces. Although, due to its minute proportion, Cr carbides could not be detected at the interfaces. The nDiamond particles appeared equiaxed and homogeneously dispersed (see arrows), with sizes in the 10-30 nm range. The nanocomposite exhibited apparent bonding at the interfaces between the carbon phase and the copper matrix.

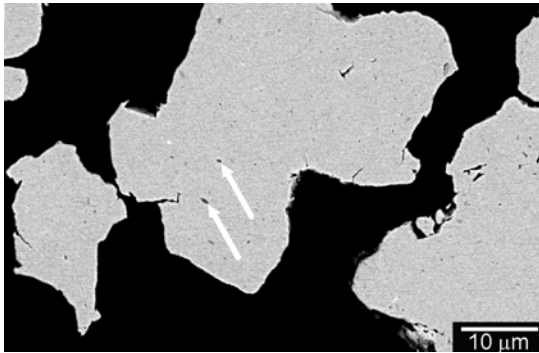


Fig. 2 BSE image of the microstructure of Cu/Cr/nDiamond as-milled powder after 8h of milling (arrows point to Fe,Cr-rich inclusions).

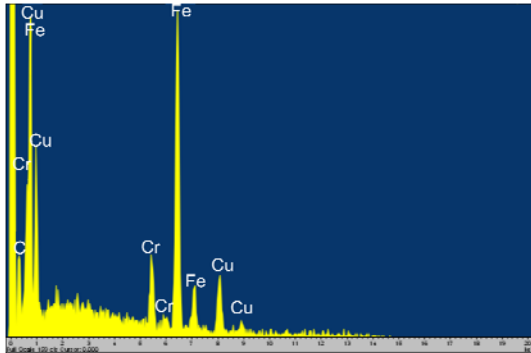


Fig. 3 EDS analysis of a typical inclusion.

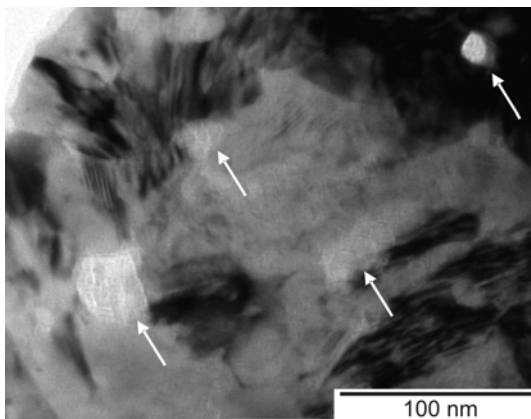


Fig. 4 TEM image of the Cu/Cr/nDiamond 600°C annealed material. The arrows point to nDiamond particles at grain boundaries and inside copper grains.

Table 1: Average composition in wt% evaluated by PIXE.

Sample	Cr	Fe	Cu
Cu/Cr/nDiamond	0.12	0.55	86.97

Fig. 5 presents the microstructure of the SPS consolidated sample. Prior particle boundaries (ppb) of the as-milled powder were bordered by pure copper (Fig. 5 (a)). This shows that plasma spark sintering induced melting of thin surface layers, which bonded the powder particles. The nDiamond particles continued to be homogeneously dispersed throughout copper matrix, while porosity could not be detected (Fig. 5 (b)). The nDiamond particles showed sizes in the 20-50 nm range.

The SPS consolidated sample exhibited a density of 7.89 g/cm³, representing 96% of densification, which is similar to the 99% densification obtained for analogous materials with hot extrusion [18,19].

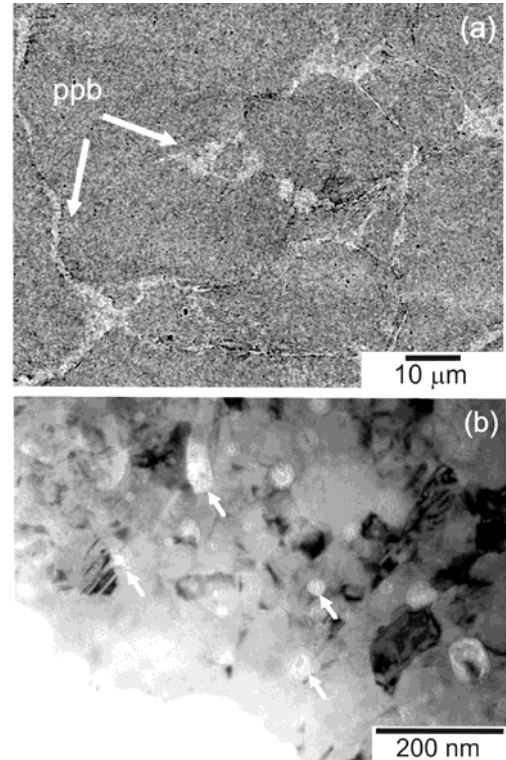


Fig. 5 (a) BSE image, and (b) TEM image of the 4h milled SPS consolidated sample. The arrows in (a) point to prior particle boundaries (ppb) and in (b) to nDiamond particles. Planar defects were observed in copper grains.

Table 2 presents the microhardness evolution of the mechanically alloyed, heat-treated and consolidated materials, together with reference values from the literature. As expected from the decrease in Cu grain size (Fig. 1), the microhardness showed a slight increase with milling time. The coarsening induced by the heat exposure during the SPS consolidation justifies the decrease in hardness relative to the as-milled powder (4h). The interfacial bonding of microdiamond dispersions in copper has been shown to increase with the presence of 0.037 at.% Cr in the matrix [20]. In the current work, since no significant microhardness difference could be detected between the Cr-doped and the non-doped nanocomposites, the level of bonding strength is not significantly enhanced with Cr doping [4]. This demonstrates that mechanical alloying is an effective bonding method for the two phases at the nanoscale. The hardness value obtained with SPS is

similar to results obtained with hot extrusion. However, the microstructural heterogeneity resulting from the thin copper films at the ppb tends to embrittle the material. In consequence, as the microstructures resulting from hot extrusion are homogeneous, this consolidation method seems preferable.

Table 2: Microhardness values of Cu/Cr/nDiamond as-milled and heat-treated powders, and SPS consolidated sample.

Cu/Cr/nDiamond*	Vickers microhardness (GPa)
Nanostructured Cu [21]	1.55
M1	3.34
M2	3.39
M4	3.52
M6	3.73
M4/without Cr doping	3.49
M4HT400	3.36
M4SPS**	2.45
M2HE [4]	2.50

* M – milling time (h), HT – heat treatment (°C), and SPS – consolidation 800°C/400MPa, and HE – Hot extrusion at 600 °C.

** The microhardness was measured at the central part of the particles, i.e., avoiding the soft ppb.

4. Conclusions

Microstructural observations showed well-dispersed nanodiamond particles in the copper matrix, displaying an apparent interfacial bonding. Optimal nanoparticle dispersion vs contamination was obtained for 4h of milling. Contaminations by the milling media can be easily monitored by particle induced X-ray emission spectroscopy. Microhardness experiments demonstrated that in the case of nDiamond dispersions effective bonding can be achieved by mechanical alloying without Cr doping. Consolidation by hot extrusion leads to higher microstructural homogeneity than spark plasma sintering.

Acknowledgements

This work has been carried out within the Contract of Association between EURATOM and Instituto Superior Técnico. Financial support was also received from Fundação para a Ciência e Tecnologia in the frame of the Associated Laboratory Contract and the PTDC/CTM/100163/2008 grant.

References

[1] R. Andreani, M. Gasparotto, *Fusion Eng Design* 61 (2002) 27.
 [2] S.V. Kidalov, F.M. Shakhov, A.Ya. Vul, *Diamond Relat. Mater.* 16 (2007) 2063.
 [3] K. Yoshida, H. Morigami, *Microelect. Reliab.* 44 (2004) 303.
 [4] J.B. Correia, V. Livramento, N. Shohoji, E. Tresso, K. Yamamoto, T. Taguchi, K. Hanada, E. Ōsawa, *Mater. Sci. Forum* 587 (2008) 443.
 [5] Th. Schubert, B. Trindade, T. Weißgärber, B. Kieback, *Mater. Sci. Engineering A* 475 (2008) 39.
 [6] T. Schubert, Ł. Ciupinski, W. Zielinski, A. Michalski, T. Weißgärber and B. Kieback, *Scripta Mater.* 58 (2008) 263.
 [7] C. Suryanarayana, *Prog. in Mat. Sci.* 46 (2001) 1.

[8] I.S. Polkin, A.B. Borzov, *Adv. Perf. Mater.* 2 (1995) 99.
 [9] M Omori, *Mater Sci Eng.* A287 (2000) 183.
 [10] L. Weber, R. Tavangar, *Scripta Mater.* 57 (2007) 988.
 [11] V. Livramento, J. B. Correia, N. Shohoji, E. Ōsawa, *Diamond Relat. Mater.* 16 (2007) 202.
 [12] J. B. Correia, H. A. Davies and C. M. Sellars, *Acta mater.* 45 (1997) 177.
 [13] P. Van Espen, K. Janssens, I. Swentens, AXIL, X-ray Analysis Software - User Manual, Canberra Packard, Benelux (1986).
 [14] M.A. Reis, L.C. Alves, A.P. Jesus, *Nucl. Instr. and Meth. B* 109/110 (1996) 134.
 [15] J.B. Correia, M.T. Marques, P.A. Carvalho, R. Vilar, *J. Alloys Comp.* 434 (2007) 301.
 [16] P.A. Carvalho, I. Fonseca, M.T. Marques, J.B. Correia, A. Almeida, R. Vilar, *Acta Mater.* 53 (2005) 967.
 [17] M.T. Marques, J.B. Correia, R. Vilar: *Rev. Adv. Mater. Sci.* 18 (2008) 403.
 [18] K. Hanada, K. Yamamoto, T. Taguchi, E. Ōsawa, M. Inakuma, V. Livramento, J.B. Correia, N. Shohoji, *Diamond Relat. Mater.* 16 (2007) 2054.
 [19] D. Nunes, V. Livramento, J.B. Correia, K. Hanada, P.A. Carvalho, R. Mateus, N. Shohoji, H. Fernandes, C. Silva, E. Alves, E. Ōsawa, *Mater. Sci. Forum* 636-637 (2010) 682.
 [20] B. Dewar, M. Nicholas, P.M. Scott, *J. Mater. Sci.* 11 (1976) 1083.
 [21] M.Y. Pan, M. Gupta, A.A.O. Tay, K. Vaidyanathan, *Microelect. Reliab.* 763 (2006) 46.